Evaluating Different Diaphragm Design Procedures Using Nonlinear 3D Computational Models

Gengrui Wei[1], Hamid Foroughi[2], Shahab Torabian[3], Benjamin W. Schafer[4], and Matthew R. Eatherton[5]

[1] Graduate Research Assistant, Dept. of Civil Engineering, Virginia Tech, gwei1@vt.edu

[2] Graduate Research Assistant, Dept. of Civil Engineering, Johns Hopkins University, hforoug1@jhu.edu

[3] Associate Research Scientist, Dept. of Civil Engineering, Johns Hopkins University, storabian@jhu.edu

[4] Professor, Dept. of Civil Engineering, Johns Hopkins University, schafer@jhu.edu

[5] Associate Professor, Dept. of Civil Engineering, Virginia Tech, meather@vt.edu

ABSTRACT

Compared to vertical elements of the seismic force resisting systems, our understanding of the horizontal elements, i.e. the diaphragms, is grossly lacking. Recent research showed that the diaphragm design forces that have been in the building codes for decades are not sufficiently large to protect the diaphragm from inelastic actions. That research led to the development of the alternative diaphragm design provisions in ASCE 7-16 which use larger diaphragm force demands, but also allows reduction by a diaphragm response modification factor, R_s, that accounts for diaphragm ductility. In this paper, the effect of different diaphragm designs on the dynamic behavior of steel buildings is studied including consideration of nonlinear behavior in both the vertical and horizontal elements of the seismic force resisting system. Three different diaphragm design scenarios are investigated: 1) a conventional design using traditional diaphragm forces from ASCE 7-16 and typical floor assemblies that are selected based on fire rating and have some overstrength, 2) diaphragms that have a strength equal to the seismic demand divided by the resistance factor ϕ based on either the traditional diaphragm forces or those calculated using the alternative diaphragm design procedures considering some ductility ($R_s = 3.0$), and 3) diaphragms with strength that is scaled to the seismic demand divided by the resistance factor ϕ based on the alternative diaphragm design procedures considering no ductility ($R_s = 1.0$). Both one-story and four-story steel buildings are included in the study with the vertical system consisting of buckling restrained braced frames. Computational models are three-dimensional assemblies of frame elements and truss elements that are capable of capturing yielding of the buckling restrained braces, plastic hinging of the beams and columns, nonlinear behavior of the diaphragm and geometric nonlinearity (i.e. second order effects). The nonlinear behavior of the diaphragm is captured using truss elements with calibrated hysteretic behavior to match past test data from cantilever diaphragm tests. The buildings were subjected to three scale levels of seismic hazard with 22 bi-directional ground motion pairs from the FEMA P695 far-field set. Two key findings include: 1) inelasticity in the diaphragm can be driven by higher modes even if the first mode pushover behavior suggests inelasticity in the vertical system will protect the diaphragm, and 2) there appears to be an interaction between inelasticity in the vertical system and diaphragm especially at large drifts where the P-delta effect exacerbates drifts.

Keywords: nonlinear three-dimensional building models, diaphragm design procedures, nonlinear response history analysis, steel deck diaphragms, buckling-restrained braced frames

1. INTRODUCTION

Steel building systems with braced frames, steel deck roof diaphragms and composite concrete on metal deck floor diaphragms are one of the most common structural systems in North America. During an earthquake, lateral inertial forces are transferred through the diaphragms to the vertical portions of the lateral force resisting system (LFRS). Conventional seismic design of these steel buildings assumes that the vertical elements of the LFRS control the dynamics of the building and that they are also the primary source of inelastic actions and hysteretic energy dissipation in the structure. However, it has been shown that diaphragms designed using traditional design procedures may be subject to inelasticity during design level earthquakes [1], and in the extreme may experience collapse such as happened for several concrete parking garages with precast concrete diaphragms during the 1994 Northridge earthquake [2].

Current U.S. seismic design provisions ASCE 7-16 [3] provide two categories of design methodologies for seismic design of diaphragms: traditional diaphragm design procedures using forces reduced by the response modification factor, R, associated with the vertical system, and alternative diaphragm design procedures using larger and presumably more accurate design forces. The alternative diaphragm design procedures incorporate a diaphragm response modification factor, R_s, that reduces the

diaphragm demands based on the ductility and overstrength in the diaphragm, but there is no R_s factor currently available for steel deck or concrete on metal deck diaphragms.

To explore the impact of different diaphragm design procedures on the seismic performance of building systems, a computational study using three-dimensional (3D) building models that capture nonlinear diaphragm behavior and its interaction with the nonlinear vertical SFRS was conducted. This paper presents details of the study starting with definition of the one-story and four-story archetype buildings with buckling-restrained braced frames (BRBF) for the vertical system and three designs for the diaphragms. The modeling scheme capitalizes on the computational efficiency of calibrated frame and truss elements to capture the realistic nonlinear behavior of both the BRBFs and the diaphragms. Nonlinear static pushover analyses and response history analyses using 44 ground motions scaled to three hazard levels are performed to investigate the behavior and seismic performance of the buildings.

2. ARCHETYPE BUILDING DEVELOPMENT

Both one-story and four-story buildings were designed using current provisions and developed as archetype buildings for the study. The buildings all use same plan dimensions, shown in Figure 1, of 300 feet by 100 feet with a story height of 14 feet at the first story and 12.5 feet for a typical story. Bare steel deck was used at the roof with loads equal to 42 psf dead load and 20 psf live load, and steel deck with concrete fill diaphragms are used for the floors with 85 psf deal load and 50 psf live load. The archetype buildings are assumed to be located in an arbitrary site in Irvine, California, with risk category II and site class D. The design spectral accelerations at short periods and at a 1-second period are 1.030g and 0.569g, respectively. More details of the archetype buildings can be found in [4].

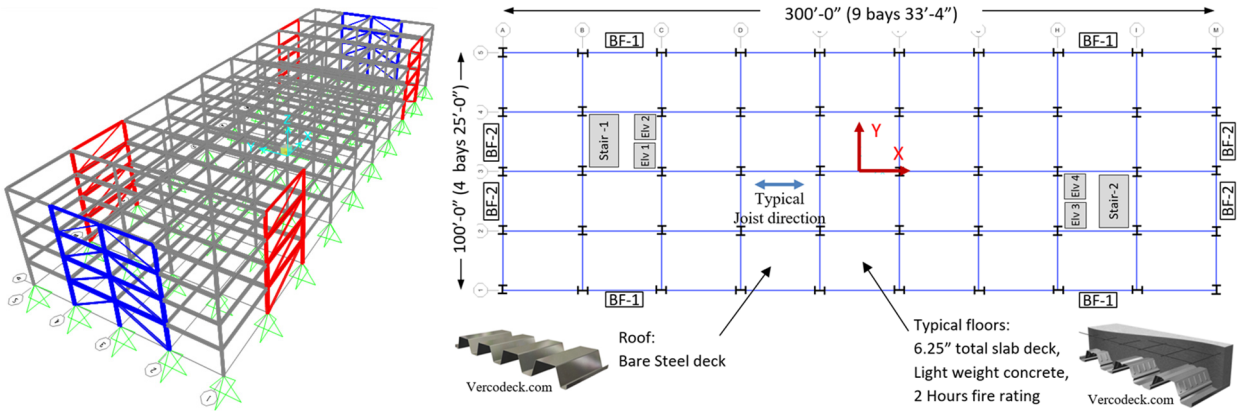

(*a*) (*b*)

Figure 1. Schematic view of four-story archetype building: (a) 3D view, (b) typical plan

Four bays of BRBFs are located on the perimeter of the building in each orthogonal direction and the diaphragm design forces are calculated three ways as tabulated in Table 1. The baseline diaphragm design uses the traditional design forces in Section 12.10.1 of ASCE 7-16 where the diaphragm design forces are based on the forces in the vertical LFRS that have been reduced by the response modification factor, R. The alternative diaphragm design provisions of Section 12.10.3 in ASCE 7-16 were used with $R_s = 1.0$ and $R_s = 3$. Table 1 shows that the baseline diaphragm force demands are the same for the alterative diaphragm design provisions with $R_s = 3$, and indeed this will be true for this archetype building with any value of $R_s \geq 1.9$ because both have the same lower bound.

Table 1. Diaphragm Design Forces for Different Design Procedures (per unit length along short direction of building, in kN/m)

Archetype Building	Level	Diaphragm Design Procedure		
		Traditional	$R_s = 1.0$	$R_s = 3.0$
one-story	2nd Level	19.11	30.57	19.11
four-story	Roof	19.11	30.57	19.11
	4th Level	38.26	62.03	38.26
	3rd Level	38.26	66.67	38.26
	2nd Level	38.26	71.31	38.26

3. MODELING SCHEME DEVELOPMENT

Computational models of the archetype buildings were created in the software, *OpenSees* [5], with nonlinear elements in the vertical LFRS and diaphragm that are calibrated against experimental test results. The models use frame and truss elements to reduce the computational cost and both material and geometric nonlinearities are considered.

3.1. Modeling of diaphragms and buckling-restrained braces

A simplified truss element model was developed to simulate diaphragm behavior in the archetype buildings. The hysteretic behavior of a diaphragm is typically obtained through cantilever diaphragm tests in which a steel deck diaphragm with or without concrete fill is supported with one edge fixed and the parallel edge subjected to a shear loading (Figure 2a). Using the force-displacement data from this type of test, a computational model with diagonal nonlinear truss elements of unit cross-section area (Figure 2b) was calibrated to capture the behavior of the diaphragm. All connections were assumed to be pinned.

The cantilever diaphragm test database established by O'Brien et al [6] was utilized as a tool to help select specimens for diaphragm material model calibration. For the roof diaphragm, the specimen of Test 33 by Martin [7] with 20-gage P3615 1.5 in. B-deck was found to have enough design strength to match the demand for the baseline archetype building roof diaphragm (herein denoted as SP1). For the floor diaphragm, test specimen 3/6.25-4-L-NF-DT was used from an ongoing testing program [8], which consisted of 3 in. deck, with lightweight concrete fill and 6.25 in. total thickness (herein denoted as SP2).

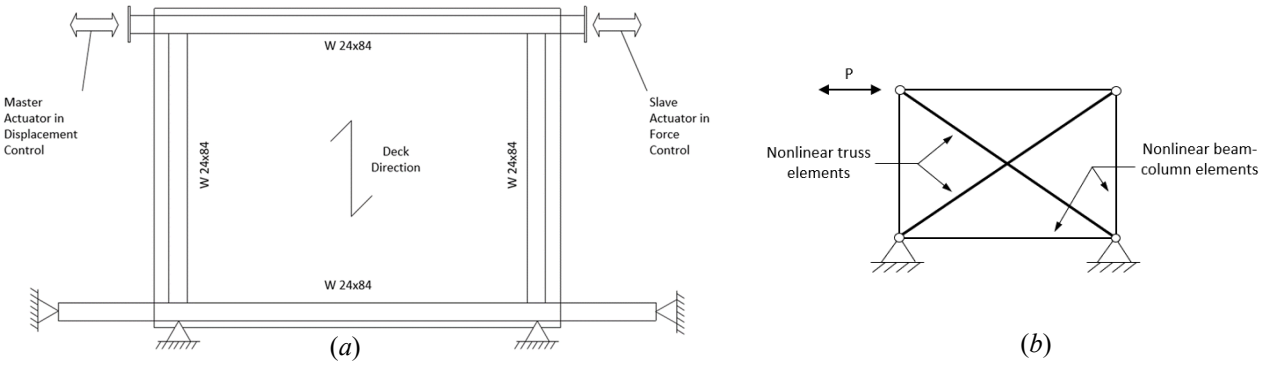

Figure 2. Cantilever diaphragm test: (a) schematic view of SP2 test setup, (b) computational model

The Pinching4 material model in *OpenSees* was used for the truss elements which is capable of capturing the hysteretic pinching, cyclic strength degradation, and cyclic stiffness degradation behavior of diaphragms. Material parameters for the Pinching4 model, including backbone stresses and strains and cyclic strength and stiffness degradation parameters, were calibrated through an optimization algorithm to achieve an optimal match between hysteretic response from the simulation and test. Table 2 shows the values of the Pinching4 material model parameters for the two selected diaphragm specimens; a detailed description of these parameters can be found in the *OpenSees* user manual [9]. Because the dimensions of the archetype building diaphragm units do not coincide with those of the test specimens, a strategy described in [10] is adopted to modify the backbone parameters so that the diaphragm shear strength per unit length is consistently represented. A comparison of the hysteretic response from the calibrated diaphragm simulation and that from the experiment is shown in Figure 3.

Table 2. Calibrated Pinching4 Material Model Parameters

Test	Backbone				Pinching			Strength Degradation					Stiffness Degradation					Energy Dissipation
	ε_1, σ_1 (MPa)	ε_2, σ_2 (MPa)	ε_3, σ_3 (MPa)	ε_4, σ_4 (MPa)	r_{Δ^+}, r_{Δ^-}	r_{P^+}, r_{P^-}	u_{Δ^+}, u_{Δ^-}	gF_1	gF_2	gF_3	gF_4	gF_{lim}	gK_1, gD_1	gK_2, gD_2	gK_3, gD_3	gK_4, gD_4	gK_{lim}, gD_{lim}	gE
SP1	0.0008, 152.9	0.0017, 199.2	0.0033, 211.6	0.0053, 165.3	0.20, 0.35	0.20, 0.35	0.10, 0.12	0	0.35	0	0.70	0.90	0, 0	0, 0.50	0, 0	0, 0.75	0, 0.90	4.31
SP2	0.0005, 437.6	0.0006, 526.8	0.0014, 740.5	0.014, 333.2	-0.06, -0.06	0.12, 0.12	0.11, 0.11	0	0.83	0.0	0.46	0.33	1.09, 0.14	0.76, 0.47	0.32, 0.12	0.75, 0.10	1.04, 0.61	4.29

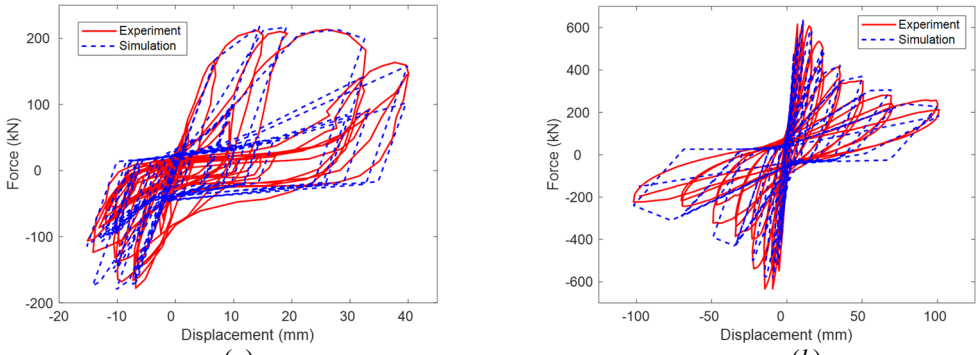

Figure 3. Hysteretic response of diaphragm from experiment and simulation: (a) SP1, (b) SP2

For each of the two archetype building heights (one-story and four-story), three building models were created with the following diaphragm designs:

i. Baseline. A baseline design using the traditional diaphragm forces from ASCE 7-16 and typical floor assemblies that are selected based on a two-hour fire rating. Cantilever diaphragm test specimen SP2, which was used in the calibration of the hysteretic model, satisfies such fire rating and is thicker than necessary for the traditional diaphragm design forces given in Table 1, thus it has some overstrength.
ii. Alternative Design 1. This design is intended to examine building behavior if the diaphragms have a strength exactly equal to the seismic demand divided by the resistance factor ϕ. In this case, the seismic demands were taken as the traditional diaphragm forces or those from the alternative diaphragm design procedures considering some ductility (R_s = 3.0), the two are equal. The hysteretic backbone was scaled accordingly.
iii. Alternative Design 2. For this model, the hysteretic backbone of the diaphragms was scaled to have a strength equal to the seismic demand divided by the resistance factor ϕ, where the seismic demand is calculated using the alternative diaphragm design procedures considering no ductility (R_s = 1.0).

For Alternative Design 1 and 2, the same Pinching4 model parameters as Baseline Design were used except that the backbone stresses were scaled so that the peak strength from hysteretic model equals the diaphragm shear demand from design. These cases assume no overstrength of the diaphragm. The scale factors for scaling backbone stresses in the four-story building for Alternative Design 2 were found to be 1.02, 0.96, 0.89, and 1.22 for the diaphragm on the 2nd, 3rd, 4th and roof level, respectively.

Similar to the calibration of diaphragm elements, a computational model for the buckling restrained brace (BRB) was also developed. As shown in Figure 4a, the BRB core (restrained yielding segment) is represented by a nonlinear truss element with Steel02 material model in *OpenSees* [11], the non-yielding segments on both ends are modeled with elastic beam-column elements, and another elastic beam-column element with negligible cross-section area and large bending stiffness is also used to connect the non-yielding segments to fix the rotational degrees of freedom and prevent instability of the truss element. The calibration of the BRB core material model has been conducted by Eatherton et al. [12] to match the behavior of a specimen tested by Fahnestock et al. [13], and the same material model is used in this study. Figure 4b shows the hysteretic curves of the calibrated model as compared to the test results.

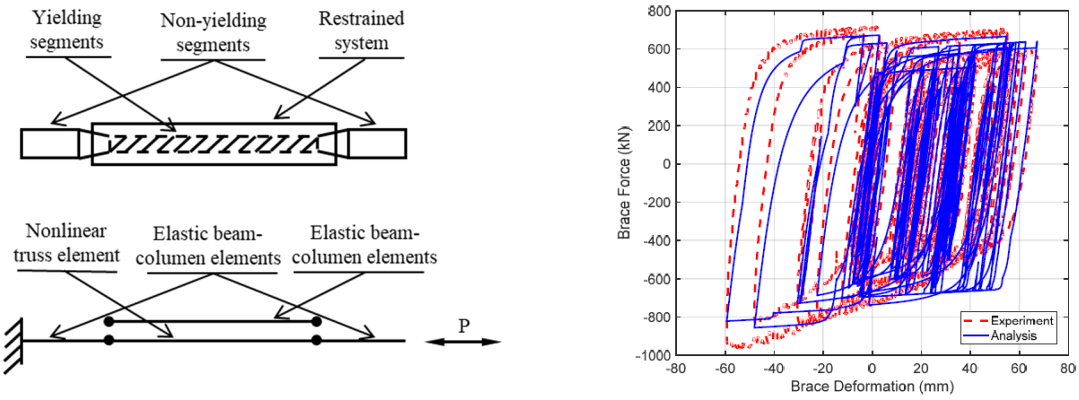

(*a*) (*b*)

Figure 4. BRB computational model: (a) configuration of a typical BRB and the computational model, (b) hysteretic curves for calibration (adapted from [12])

3.2. Other modeling details

3D models with the previously described calibrated nonlinear diaphragm and BRB elements were created and isometric views of the models are presented in subsequent sections. Some additional details of the models include:

1) Boundary conditions and joint fixity. All columns were pinned at the base and continuous over the building height. All the beam-to-column and beam-to-beam joints were pinned except for the beam-to-column joints of the BRB frames which were made rigid for all degrees of freedom. The reason for making these connections rigid is that in practice these connections have substantial gusset plates, welds and/or bolts that make them effectively act as a moment connection.
2) Gravity loads and masses. As recommended by FEMA P695 [14] the gravity loads included a combination of dead loads and live loads (1.05D+0.25L). Masses were determined from the dead loads and lumped at the column nodes on each floor.
3) Material and geometric nonlinearity. Both material and geometric nonlinearity were considered in the analysis. In addition to the aforementioned nonlinear material models of diaphragms and BRB's, the columns and beams were represented by

nonlinear beam-column elements with fiber-section formulation. Geometric nonlinearity was considered by including the gravity loads and using the P-Delta coordinate transformation algorithm in *OpenSees* for the columns.

4) Damping. For nonlinear response history analysis, Rayleigh damping with a critical damping ratio equal to 2% for the 1st and 2nd mode is used for the archetype building models.

4. ANALYSES RESULTS

The 3D models of the archetype buildings were used to conduct different types of analyses. Eigenvalue analysis was performed to study the modal properties of the structures. Nonlinear static pushover analysis was performed to investigate their streng and expected failure mode. Then, nonlinear response history analyses were conducted with a suite of ground motions at different scale level to evaluate the seismic performance of the archetype buildings with the three diaphragm designs.

4.1. Eigenvalue analysis

Eigenvalue analysis was performed for the one-story and four-story archetype buildings in *OpenSees* to obtain their natural periods and mode shapes. To study the effect of the rigid diaphragm assumption on modal properties of the building structure, linear elastic models were also created using the commercial structural analysis program *SAP2000* for the building framing members using rigid diaphragm constraints. Table 3 provides the 1st and 2nd periods of the archetype buildings obtained from eigenvalue analysis of the models in *OpenSees* that uses an elastic diaphragm and *SAP2000* that uses a rigid diaphragm. Figure 5 shows the mode shape for the 1st mode of four-story archetype models. It can be observed that diaphragm deflections can have a substantial effect on building natural period (66% larger than rigid) and on the mode shape shown in Figure 5a which shows potential for a "whipping effect" at the roof due to roof diaphragm flexibility.

Table 3. Natural Periods of Archetype Models in OpenSees and SAP2000

Building Model		1st Mode (sec)	2nd Mode (sec)
one-story	Elastic Diaphragm	0.98	0.59
	Rigid Diaphragm	0.52	0.46
four-story	Elastic Diaphragm	1.13	1.10
	Rigid Diaphragm	0.94	0.76

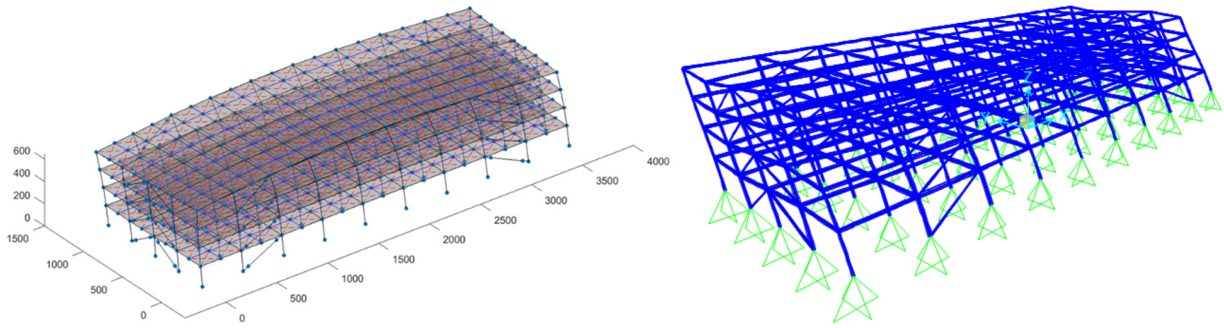

(*a*) (*b*)

Figure 5. Mode shapes for the 1st mode of four-story archetype models: (a) OpenSees model, (b) SAP2000 model

4.2. Pushover analysis

Pushover analysis was conducted to study the static behavior of archetype buildings. A displacement-controlled load pattern was applied to the structure in the short direction (long diaphragm span direction). Per FEMA P695, vertical distribution of the lateral force at each node was assigned proportional to the product of the tributary mass and the fundamental mode shape coordinate at the node.

Figure 6a and 6b show the pushover curves of the one-story and four-story archetype buildings, respectively, with different diaphragm designs. These curves are plotted up to the limits of the model, defined as when the BRB strains or the diaphragm shear angles exceed the maximum values from the calibration tests which were 0.0338 mm/mm, 0.0110 rad. and 0.0275 rad. for the BRB, roof diaphragm (SP1), and floor diaphragm (SP2), respectively. The drift ratio was calculated as the applied displacement at the center of the roof divided by the building height. It can be observed that the different diaphragm design procedures have a small impact on the pushover curves of the archetype buildings because the yielding is associated with the BRB's. The first point of nonlinearity on the pushover curves is associated with yielding of the BRB cores. For one-story archetype models, this is followed by a hardening segment with reduced slope, which is related to the stiffness provided by the BRB frames before hinging occurs at the beam-to-column connections. For the four-story models, because the BRB yielding first occurs at the first story where the story shear is the largest, the forces acting on the BRB frames are also large after the

BRB's yield, which causes the hinging of beam-to-column connections to occur much faster and thus no hardening segment is observed. The post-peak softening segment of the pushover curves are attributed to P-Δ effect which controls over the BRB material hardening.

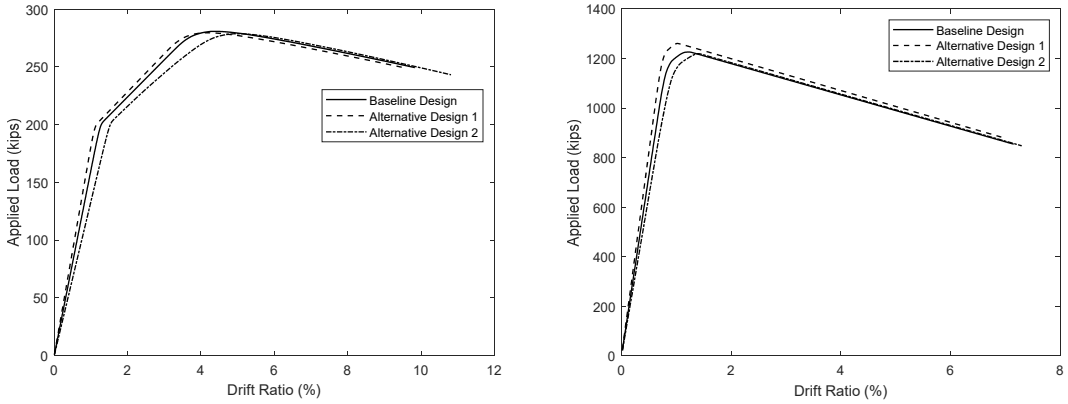

Figure 6. Pushover curves of archetype buildings with the three diaphragm design procedures: (a) one-story, (b) four-story

4.3. Nonlinear response history analyses

To evaluate the seismic performance of the archetype buildings with different diaphragm design procedures, nonlinear response history analysis was performed with the archetype models subjected to the suite of FEMA P695 far-field earthquake motions. Three scale levels are considered for nonlinear response history analysis:

- Design earthquake (DE)
- Maximum considered earthquake (MCE)
- A scale level based on adjusted collapse marginal ratio ($ACMR_{10\%}$, see FEMA P695)

The 22 pairs of ground motions are scaled accordingly to each desired level and are applied in orthogonal directions of the building in the analysis (two possible orientations of each pair result in 44 total sets of analysis for each archetype building model). For DE and MCE, the ground motions are scaled such that the median spectrum matches the design spectrum at the fundamental period of the building. To be consistent with FEMA P695 methodology, the value of the fundamental period is obtained by the product of the coefficient for upper limit on calculated period (C_u) and the approximate fundamental period (T_a) as defined in ASCE 7-16 Section 12.8.2, which is 0.30 second for one-story and 0.81 second for four-story archetype building. For the third level, the scale factor is obtained with similar methodology described in FEMA P695 but done backward: first an acceptable value of adjusted collapse margin ratio ($ACMR_{10\%}$) is obtained with assumed total system collapse uncertainty ($\beta_{TOT} = 0.525$); then the period-based ductility (μ_T) is obtained from the pushover analysis; and finally the spectral shape factor (*SSF*) and collapse margin ratio (*CMR*) is obtained. The scale factor based on $ACMR_{10\%}$ is then obtained by multiplying the collapse marginal ratio by the scale factor for MCE. If less than half of the ground motions at this scale level cause the archetype buildings to collapse, then the seismic performance will be deemed satisfactory. Based on the procedures, the scale factors for the three levels considered are provided in Table 4. Note that a reduction factor of 1.2 for the scale factors based on $ACMR_{10\%}$ was included for nonlinear 3D analysis per FEMA P695.

Table 4. Scale Factors for Unscaled Far-Filed Ground Motion Record Set in Nonlinear Response History Analysis

Archetype Building	DE	MCE	$ACMR_{10\%}$
one-story	1.29	1.94	2.46
four-story	1.67	2.50	3.07

Figure 7 shows some example response history results with peak story drift and BRB force-deformation hysteresis of archetype buildings with the Baseline Design subjected to the ground motion recorded at Delta Station during the 1979 Imperial Valley Earthquake with DE and MCE scales. The BRB's undergo inelastic deformation under ground motions at both scales. However, the buildings subjected to the MCE scaled ground motion experience ever increasing story drifts indicating that the buildings collapse. Figure 8 shows the deformed shapes of the archetype buildings subjected to MCE scale ground motions. Unlike the first-mode based pushover analysis in which inelasticity focuses in the BRB's, the participation of higher modes in the response history analysis leads to diaphragm inelasticity. As shown in Figure 8, the total story drifts include inelastic deformations in the vertical LFRS and the diaphragm such that the two compound each other (i.e. interact) to exacerbate the P-Δ effect which eventually leads to the collapse of the buildings.

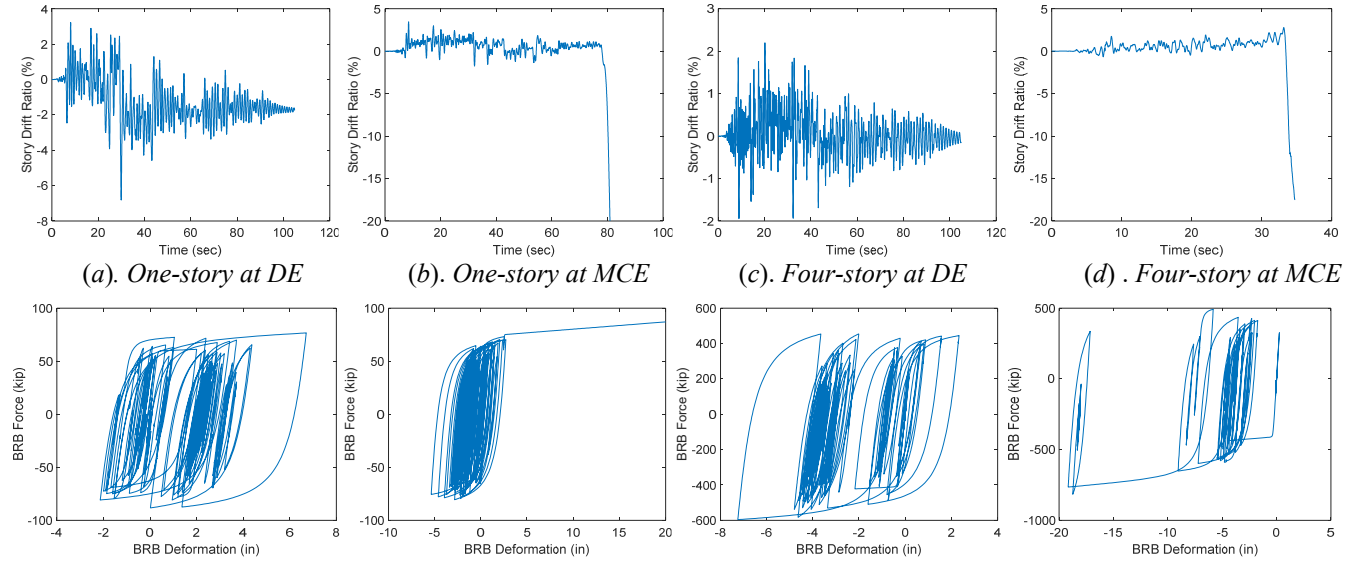

(*a*). *One-story at DE* (*b*). *One-story at MCE* (*c*). *Four-story at DE* (*d*) . *Four-story at MCE*

Figure 7. Example time history response with peak story drift and BRB hysteresis of archetype buildings with Baseline Design

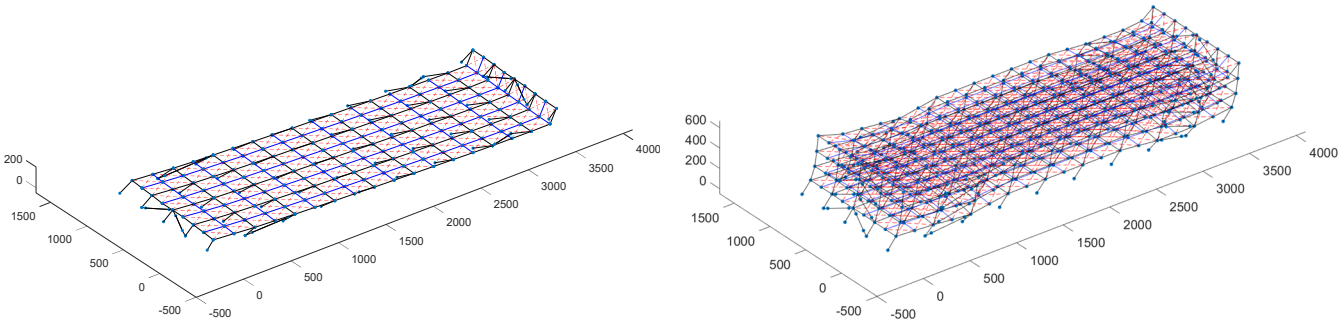

Figure 8. Deformed shapes of archetype buildings under MCE-level ground motions (deformation amplification factor: 10)

Peak story drift ratio (SDR) is one measure to quantify the seismic performance of buildings. Table 5 provides the values of median peak SDR and probability of SDR exceeding 10% for archetype buildings from all response history analyses (note that those which fail to converge in the analysis are also considered to have a peak SDR exceeding 10%). When diaphragm deflections are considered, the median peak SDR is found to be quite large (3% to 4% for DE and 5% to 6% for MCE) compared to DE level story drift limits in ASCE 7-16 (2%). Furthermore, it is noted that more than half of the runs with $ACMR_{10\%}$ scale motions for the four-story building with Alternative Design 1 experienced a peak SDR greater than 10%, which demonstrates an unsatisfactory collapse-prevention performance if this peak SDR exceedance is considered as a sign for collapse. For Alternative Design 1, the strength of the diaphragm elements was scaled to be exactly equal to the required strength for traditional diaphragm forces or those from the alternative diaphragm design provisions with $R_s = 3.0$. These results indicate that typical conventional buildings with some built in diaphragm overstrength are expected to experience story drifts substantially larger than expected from analysis of the vertical LFRS alone, and that buildings where the diaphragms don't have any overstrength above the current diaphragm force demands may be subject to collapses beyond what is allowed in FEMA P695.

Table 5. Median Peak SDR and Probability of Peak SDR Exceeding 10%

Archetype Building	Ground Motion Scale	Median Peak SDR (%)			Probability of Peak SDR > 10% (%)		
		Baseline	Alt. 1	Alt. 2	Baseline	Alt. 1	Alt. 2
one-story	DE	3.47	3.57	3.18	0.0	0.0	0.0
	MCE	5.35	5.41	5.26	9.1	9.1	4.5
	$ACMR_{10\%}$	7.11	7.68	6.77	27.3	36.4	27.3
four-story	DE	3.59	3.92	3.32	4.5	15.9	0.0
	MCE	5.21	6.28	5.19	18.2	34.1	18.2
	$ACMR_{10\%}$	6.99	7.12	6.92	38.6	68.2	34.1

5. CONCLUSIONS

A series of one-story and four-story archetype buildings were designed to the current U.S. building code with three different diaphragm designs: a baseline design that uses traditional diaphragm design forces and typical floor and roof assemblies that have some overstrength, an alternative design that uses diaphragm strength exactly equal to the seismic demand from either the traditional diaphragm forces or those calculated assuming some diaphragm ductility (R_s = 3.0), and an alternative design with diaphragm strength scaled to demands assuming no diaphragm ductility (R_s = 1.0). Using material models calibrated against test data for diaphragms and BRB, 3D computational models with material and geometric nonlinearity were created. These models were used to conduct eigenvalue analyses to study their modal properties, pushover analyses to investigate their static behavior, and nonlinear response history analyses to evaluate their seismic performance. It was found that design office models with a rigid diaphragm assumption can significantly underpredict the natural period (up to 66% underpredicted for some models) and miss some key features of the mode shape. The different diaphragm designs had little effect on the pushover behavior because the pushover analyses used a first mode shape based load pattern and as such were dominated by BRB inelasticity. Conversely, response history analyses showed significant inelasticity occurred in the diaphragms as higher modes affected the diaphragm demands. There was also an interaction between diaphragm inelasticity and BRB inelasticity as the two compounded each other to exacerbate the second order effects and cause collapse. Peak story drifts calculated including diaphragm deflections were considerably larger (3% to 4%) than the code prescribed limit on story drift (2%). Furthermore, the results suggest that buildings with no diaphragm overstrength as compared to the design diaphragm forces, may not satisfy the FEMA P695 collapse criteria. This study identifies important issues related to diaphragm design, but more study is required to determine which diaphragm design procedures or values of R_s are appropriate.

ACKNOWLEDGMENTS

This work was supported by the National Science Foundation under Grant No. 1562669 and the Steel Diaphragm Innovation Initiative which is funded by AISC, AISI, SDI, SJI, and MBMA. The Advanced Research Computing (ARC) at Virginia Tech provided high-performance computing resources which facilitated the computational study. Any opinions expressed in this paper are those of the authors alone, and do not necessarily reflect the views of the National Science Foundation.

REFERENCES

[1] Rodriguez, M., Restrepo, J., and Blandón, J. (2007). Seismic design forces for rigid floor diaphragms in precast concrete building structures. *Journal of Structural Engineering*, 133(11), pp. 1604–1615.

[2] EERI (1996). Northridge Earthquake Reconnaissance Report, Vol. 2 Earthquake Spectra - Supplement C to Volume 11 Earthquake Engineering Research Institute.

[3] American Society of Civil Engineers. (2016). Minimum design loads for buildings and other structures (ASCE standard). Reston, Va.: American Society of Civil Engineers.

[4] Torabian, S., Eatherton, M.R., Easterling, W.S., Hajjar, J.F., Schafer, B.W. (2017) "SDII Building Archetype Design v1.0" CFSRC Report R-2017-04, permanent link: jhir.library.jhu.edu/handle/1774.2/40638.

[5] Mazzoni, S., McKenna, F., Scott, M. H., & Fenves, G. L. (2006). OpenSees command language manual. Pacific Earthquake Engineering Research (PEER) Center, 264.

[6] O'Brien, P., Eatherton, M. R., & Easterling, W. S. (2017). Characterizing the load-deformation behavior of steel deck diaphragms using past test data. Cold-Formed Steel Research Consortium Report Series, CFSRC R-2017-02.

[7] Martin, É. (2002). Inelastic response of steel roof deck diaphragms under simulated dynamically applied seismic loading. Master's thesis, Ecole Polytechnique de Montreal.

[8] Avellaneda Ramirez, R.E., Easterling, W. S., Schafer, B.W., Hajjar, J.F., and Eatherton, M.R. (2019) "Cyclic Testing of Composite Concrete on Metal Deck Diaphragms Undergoing Diagonal Tension Cracking", 12th Canadian Conference on Earthquake Engineering, Chateau Frontenac, Quebec, QC.

[9] Lowes, L. N., & Altoontash, A. (2003). Modeling reinforced-concrete beam-column joints subjected to cyclic loading. *Journal of Structural Engineering*, 129(12), 1686-1697.

[10] Qayyum, B. (2017). Computational modeling of one-story buildings with nonlinear steel deck diaphragms subjected to earthquakes. Report, Virginia Tech.

[11] Fillipou, F. C., Popov, E. P., & Bertero, V. V. (1983). Effect of bond deterioration on hysteretic behaviour of reinforced concrete joints. Report EERC 83-19. *Earthquake Engineering Research Center, University of California, Berkeley, Calif.*

[12] Eatherton, M. R., Fahnestock, L. A., & Miller, D. J. (2014). Computational study of self-centering buckling-restrained braced frame seismic performance. *Earthquake Engineering & Structural Dynamics*, *43*(13), 1897-1914.

[13] Fahnestock, L. A., Ricles, J. M., & Sause, R. (2007). Experimental evaluation of a large-scale buckling-restrained braced frame. *Journal of structural engineering*, *133*(9), 1205-1214.

[14] Applied Technology Council. (2009). *Quantification of building seismic performance factors*. US Department of Homeland Security, FEMA.